Talanta 99 (2012) 840–845

Contents lists available at SciVerse ScienceDirect

Talanta

journal homepage: www.elsevier.com/locate/talanta

# A highly sensitive and automated method for the determination of hypoxanthine based on lab-on-valve approach using $Fe_3O_4$/MWCNTs/β-CD modified electrode

Yang Wang [a,b,*], Lu Wang [a,b], Tian Tian [a,b], Guojun Yao [a], Xiaoya Hu [a], Chun Yang [a], Qin Xu [a]

[a] School of Chemistry and Chemical Engineering, Yangzhou University, Yangzhou 225002, China
[b] The Key Laboratory of Environmental Material and Engineering of Jiangsu Province, Yangzhou University, Yangzhou 225002, China

ARTICLE INFO

*Article history:*
Received 7 May 2012
Received in revised form
12 July 2012
Accepted 13 July 2012
Available online 22 July 2012

*Keywords:*
$Fe_3O_4$
Multiwall carbon nanotubes
β-Cyclodextrin
Sequential injection lab-on-valve
Hypoxanthine

ABSTRACT

A $Fe_3O_4$/multiwall carbon nanotubes/β-cyclodextrin ($Fe_3O_4$/MWCNTs/β-CD) modified electrode, for highly sensitive and automated hypoxanthine measurements, was developed in a sequential injection lab-on-valve system. The electrochemical oxidation behavior of hypoxanthine was investigated in phosphate buffer solution by cyclic voltammetry and linear sweep voltammetry. The $Fe_3O_4$/MWCNTs/β-CD modified electrode exhibits preferably analytical characteristics in electrocatalytic activity towards the oxidation of hypoxanthine. Under optimized conditions, the log oxidation peak current intensity was proportional to log hypoxanthine concentration covering the range from $5.0 \times 10^{-8}$ to $1.0 \times 10^{-5}$ mol $L^{-1}$ with a correlation coefficient of 0.9965. A detection limit of $0.3 \times 10^{-8}$ mol $L^{-1}$ was achieved along with a sampling frequency of 20 $h^{-1}$. This hyphenated system offers some advantages in terms of rapidness, sensitivity and ease of manipulation. Its further applications were utilized for the determination of hypoxanthine in meat samples.



## 1. Introduction

As one of the purine bases, hypoxanthine is produced during the degradation process of fresh meat, which suggests that hypoxanthine content can be a valuable indicator of meat freshness in the food industry [1,2]. Thus, the development of efficient, sensitive, and simple analytical techniques for the determination of hypoxanthine is important for the quality control of meat products. To date, numerous applications of electrochemical methods using modified electrodes have been developed for the determination of hypoxanthine [3–6]. Zhang et al. employed sensitive electrocatalytic biosensing based on graphene sheets with water-soluble conducting graft copolymer to determine hypoxanthine by an enzymatic cycle [7]. Lü investigated the electrochemical behavior of hypoxanthine on multiwalled carbon nanotubes (MWCNTs)-dicetyl phosphate film modified vitreous carbon electrode [8]. Xie et al. constructed a mesoporous $TiO_2$ modified carbon paste electrode and its application was used in the determination of hypoxanthine in human blood serum samples [9].

Nanomagnetic materials are expected to exhibit new functional properties for a wide range of applications, among which $Fe_3O_4$ magnetic nanoparticles have aroused researchers' interest and had been applied in electrochemical sensor [10–12]. Wang and Tan prepared a novel amperometric immunosensor based on $Fe_3O_4$ nanoparticles/chitosan composite film for determination of ferritin. The developed immunoassay was comparable with the radioimmunoassay [13]. Yu et al. and Fan et al. investigated the bioelectrocatalytic activity to the reduction of $H_2O_2$ by immobilizing hemoglobin on the surface of core-shell structure magnetic $Fe_3O_4$ nanoparticles [14,15].

MWCNT materials have attracted considerable attention due to their favorable electrical conductivity, high chemical stability, and extremely high mechanical strength [16–18]. Incorporating $Fe_3O_4$ nanoparticles onto MWCNTs could improve the electrocatalytic properties of modified electrodes [19,20]. However, the lack of solubility and the difficult manipulation in any solvents have imposed great limitations to the use of MWCNTs. β-Cyclodextrin (β-CD) is composed of a hydrophilic exterior surface and a hydrophobic interior cavity. This structural property makes it easier to form inclusion complexes with many organic compounds and readily soluble in aqueous solutions [21]. Therefore, the preparation of glassy carbon modified electrode with β-CD incorporated MWCNTs may provide a nice strategy to improve the resolvable property of MWCNTs [22,23]. However, to the best of our knowledge, a study to determine hypoxanthine using $Fe_3O_4$/MWCNTs/β-CD modified electrode has not yet been reported.

Currently, analytical laboratories experience an increasing demand for a large number of analytical determinations. Most procedures are

* Corresponding author at: School of Chemistry and Chemical Engineering, Yangzhou University, Yangzhou 225002, China. Tel./fax: +86 514 87975587.
*E-mail address:* wangyangyz@yahoo.cn (Y. Wang).

0039-9140/$ - see front matter © 2012 Elsevier B.V. All rights reserved.
http://dx.doi.org/10.1016/j.talanta.2012.07.040

laborious and generally time-consuming and thus may not be appropriate for the required laboratory productivity. The above mentioned problems can be solved by implementing in an easy and inexpensive way by means of the sequential injection lab-on-valve (SI-LOV) technique [24–27], in which all necessary laboratory facilities for on-line manipulation could be integrated within the LOV unit. These features made this system most suitable for automatic purposes. The aim of this work was to investigate the possibility of application of $Fe_3O_4$/MWCNTs/β-CD modified electrode for hypoxanthine determination in the dynamic SI-LOV system. Various experiments were conducted to establish the optimum analytical conditions. For further confirmation of the feasibility of practical application, the hypoxanthine contents in real meat samples were determined.

## 2. Experimental

### 2.1. Apparatus

Voltammetric measurements were performed with a CHI660A electrochemical workstation (Chenhua Instrument, Shanghai, China). A sequential injection system (Cavro, Sunnyvale, CA, USA) equipped with a 24,000-step syringe pump with a capacity of 2.5 mL and a six-port selection valve was employed for solutions delivery. A homemade LOV unit incorporated an electrochemical flow cell (EFC) consisting of a 2.0 mm glassy carbon electrode (GCE) as working electrode, a 0.5 mm platinum wire as counter electrode and a 1.0 mm Ag/AgCl as reference electrode. The central channel was connected to 2500 μL high-precision syringe pump via holding coil. Ports 1 and 2 were used as reserved channels. All the used tubes were made of 0.8 mm i.d. PTFE tubing (Upchurch Scientific, OakHarbor, WA, USA). Static contact angle measurements were carried out at 20 °C with a sessile drop method using a CAM200 optical contact angle analyzer (KSV Instruments, Finland). The HPLC apparatus (Shimadzu, Kyoto, Japan) with a SPD-10A VP UV–visible (UV–vis) detector was used for chromatographic separation and determination of hypoxantine. Scanning electron micrographs (SEM) were obtained with a Hitachi S-4800 scanning electron microscope (Japan) at an acceleration voltage of 15 kV.

### 2.2. Reagents and materials

A stock standard solution ($1.0 \times 10^{-3}$ mol $L^{-1}$) of hypoxanthine was prepared in 0.1 mol $L^{-1}$ NaOH and working standard solutions were obtained by appropriate stepwise dilution of the stock standard solution with deionized water. Phosphate buffer solution (PBS) was prepared by mixing the stock solution of 0.1 mol $L^{-1}$ $NaH_2PO_4$ and 0.1 mol $L^{-1}$ $Na_2HPO_4$ and adjusting the pH with 0.1 mol $L^{-1}$ $H_3PO_4$ or 0.1 mol $L^{-1}$ NaOH. Ferrous chloride tetrahydrate ($FeCl_2 \cdot 4H_2O$), ferric chloride hexahydrate ($FeCl_3 \cdot 6H_2O$), β-cyclodextrin, and N,N-dimethylformamide (DMF) were purchased from Sinopharm Chemical Reagent Co., Ltd. (Shanghai, China). The MWCNTs were purchased from Nanotech Port Co., Ltd. (Shenzhen, China) with an average size of 25 nm, which were purified by stirring the MWCNTs in concentrated nitric acid at 60 °C for 12 h, and then dried at 110 °C for 4 h. Double deionized water (18 MΩ $cm^{-1}$) was prepared by the Milli-Q water purification system (Millipore, Bedford, MA, USA) and used as carrier stream.

### 2.3. The construction of $Fe_3O_4$/MWCNTs/β-CD modified glassy carbon electrode

The $Fe_3O_4$/MWCNTs nanocomposites were prepared by the chemical coprecipitation method after a minor modification [28]. First, 48 mg MWCNTs were dissolved in 30 mL of distilled water for 30 min with the aid of ultrasonication. Second, 40.5 mg of $FeCl_3 \cdot 6H_2O$ and 16 mg of $FeCl_2 \cdot 4H_2O$ were added to the above mixture and kept vigorously stirring for 30 min. Third, 4 mL $NH_3 \cdot H_2O$ diluted with 20 mL of distilled water was added drop by drop, and the mixtures were heated subsequently to 60 °C for 2 h. That is, $Fe^{2+}$ salt reacts with $Fe^{3+}$ salt to produce coprecipitation with a molar ratio of 1:2 under alkaline condition. After the reaction, the nanoparticles precipitate was washed 3 times with doubly distilled water and dried at 50 °C for 24 h. The whole reaction process was performed under nitrogen gas protection. Before starting the experiment, GCE was polished manually to obtain a fresh surface. 10 mg of β-CD was dispersed in 1 mL of DMF, containing 2 mg of nanoparticles to produce black suspension with the aid of ultrasonic agitation. The $Fe_3O_4$/MWCNTs/β-CD/GCE was prepared by dropping this suspension on the glassy carbon electrode surface and the solvent was allowed to evaporate at room temperature in the air.

### 2.4. Sample pretreatment

Approximately 100 g of meat samples was triturated and homogenized. Then a portion of 3.0 g was mixed with 10 mL of 0.5 mol $L^{-1}$ perchloric acid solution for about 1 h. After centrifugation, 1.0 mL of the supernatant extract was diluted to 10 mL with 0.1 mol $L^{-1}$ PBS.

### 2.5. Operating procedure

A diagram of the SI-LOV system used in this study was illustrated in Fig. 1. The entire operating processes were summarized as follows: First, 500 μL of PBS was aspirated into the holding coil. After the flow reversal, the EFC and the connecting line were conditioned. Thereafter, 400 μL of carrier, 100 μL of air, 400 μL of sample solution, and 1600 μL of PBS were aspirated into the holding coil followed by transfer into EFC at a flow rate of 16 μL $s^{-1}$, during which the analyte was accumulated onto the surface of modified electrode at a potential of −0.1 V for 120 s. Finally, the hypoxanthine was stripped with a potential range from 0.8 to 1.2 V and the stripping current was recorded.

## 3. Results and discussion

### 3.1. Characterization of $Fe_3O_4$/MWCNTs/β-CD modified electrode

The static contact angle is commonly used to characterize the relative hydrophobicity/hydrophilicity of modified glassy carbon

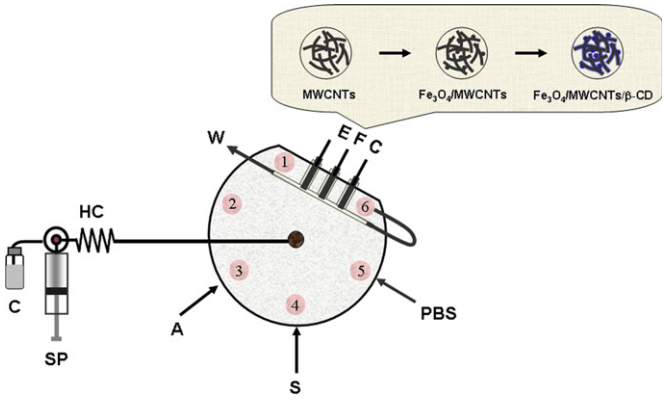


**Fig. 1.** Schematic diagram of the proposed SI-LOV manifold in conjunction with voltammetry for hypoxanthine analysis. C: carrier ($H_2O$); SP: syringe pump; HC: holding coil; W: waste; A: air; S: sample; PBS: phosphate buffer solution and EFC: electrochemical flow cell (internal volume: 200 μL).

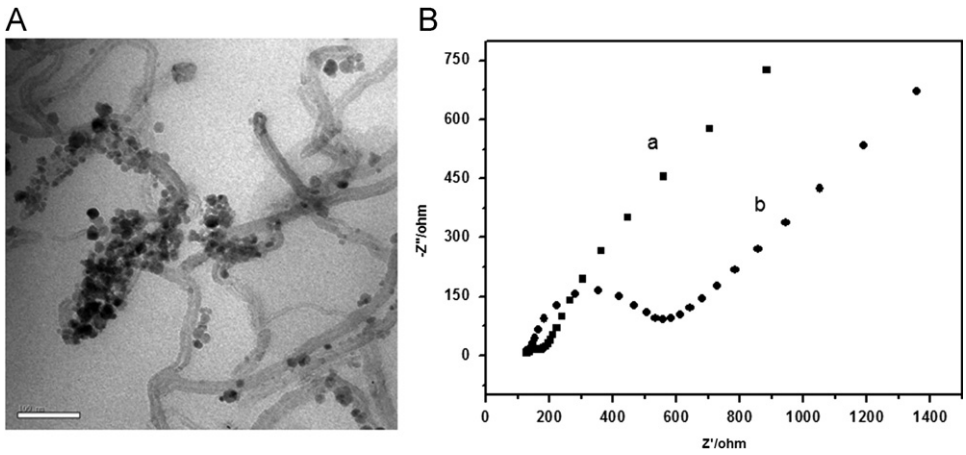


**Fig. 2.** (A) SEM image of $Fe_3O_4$/MWCNTs/β-CD nanocomposites. (B) Nyquist plots of electrochemical impedance spectroscopy for (a) bare GCE and (b) $Fe_3O_4$/MWCNTs/β-CD/GCE in $1\times10^{-3}$ mol $L^{-1}$ $Fe(CN)_6^{3-/4-}$ and 0.1 mol $L^{-1}$ $KNO_3$ solution.

electrode surface. The contact angle is measured to be 59.2° for bare glassy carbon electrode. After modifying with $Fe_3O_4$/MWCNTs, the contact angle increased (about 79°) compared to bare GCE, resulting in the hydrophobic features on the surface of $Fe_3O_4$/MWCNTs. After modifying with $Fe_3O_4$/MWCNTS/β-CD, the interface became much more hydrophilic with a contact angle of 38.7°. This phenomenon indicates the high adsorbability of $Fe_3O_4$/MWCNTs/β-CD modified electrode surface to water. Hence, the combination of $Fe_3O_4$/MWCNTs and β-CD from their individual distinct advantages revealed the potential application in the enhancement of the electron exchange.

The microstructure of the modifier was investigated by SEM in Fig. 2A. As can be seen, the diameter of $Fe_3O_4$/MWCNTs/β-CD was about 20–30 nm, and the $Fe_3O_4$ nanoparticles with an average diameter of 15 nm were attached to MWCNTs and β-CD layer was coated on the surface of MWCNTs/$Fe_3O_4$ nanocomposites.

For further characterization of the modified electrode, electrochemical impedance spectroscopy was employed to characterize the interfacial properties of the modified electrode using $Fe(CN)_6^{3-/4-}$ as the redox probe. Fig. 2B shows the impedance spectra in the form of Nyquist diagrams of bare GCE (curve a) and $Fe_3O_4$/MWCNTs/β-CD/GCE (curve b). A small well defined semicircle ($Rct=64.06\ \Omega$) at higher frequencies was obtained at the bare GCE, suggesting a low transfer resistance. When $Fe_3O_4$/MWCNTs/β-CD nanocomposite was deposited on the GCE surface, the semicircle increased ($Rct=157.2\ \Omega$), indicating the impedance of the electrode increases in the presence of $Fe_3O_4$/MWCNTs/β-CD nanocomposite film. These results demonstrated that $Fe_3O_4$/MWCNTs/β-CD nanocomposite was successfully immobilized on the GCE surface.

The surface coverage concentration ($\Gamma$ mol $cm^{-2}$) of the electroactive hypoxanthine on the electrode surface can be calculated from the charge integration of cathodic peak in cyclic voltammogram at 50 mV $s^{-1}$, according to $\Gamma=Q/nFA$, where $Q$ is the charge consumed in the reaction, $n$ is the number of electrons transferred, $F$ is the Faraday constant, and $A$ is the electrode area. The surface coverage was calculated to be $2.0\times10^{-10}$ mol $cm^{-2}$, indicating saturated adsorption of hypoxanthine in multilayers of the nanocomposite film.

### 3.2. Voltammetric studies of hypoxanthine on $Fe_3O_4$/MWCNTs/β-CD/GCE

The electrochemical behaviors of hypoxanthine ($1.0\times10^{-6}$ mol $L^{-1}$) in 0.1 mol $L^{-1}$ PBS (pH 7.5) at $Fe_3O_4$/MWCNTs/β-CD/GCE were investigated in detail by cyclic voltammetry in batchwise mode, and also compared with that at bare GCE, MWCNTs/GCE, and $Fe_3O_4$/MWCNTs/GCE. As shown in Fig. 3, the oxidation of hypoxanthine at these electrodes is totally irreversible under these experimental conditions, and a defined oxidation peak was observed at the bare electrode with a potential at 1.078 V. After the bare GCE was modified with MWCNTs, the peak current increased with a potential at 1.059 V because of the large surface area of the MWCNTs. With the application of $Fe_3O_4$/MWCNTs/GCE, the oxidation peak current of hypoxanthine increased greatly (1.043 V), which indicated that $Fe_3O_4$ nanoparticles contributed to the significant improvement of the electrocatalytic activity of the modified electrode due to their small dimension effect, the quantum size effect, and the large surface area. When β-CD was immobilized on $Fe_3O_4$/MWCNTs/GCE surface, the oxidation peak current of hypoxanthine (1.047 V) at $Fe_3O_4$/MWCNTs/β-CD/GCE was much larger compared with the other modified electrodes. This change arises from the existence of β-CD, indicating that the relatively hydrophilic surface could considerably promote the electron transfer.

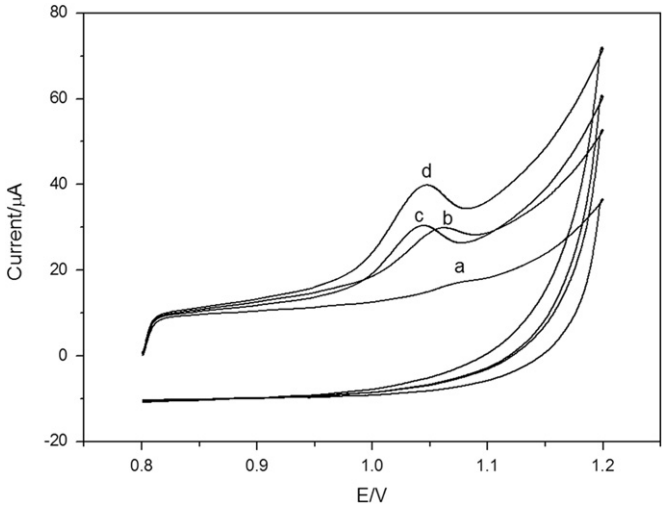


**Fig. 3.** Cyclic voltammograms at bare GCE (a), MWCNTs/GCE (b), $Fe_3O_4$/MWCNTs/GCE (c) and $Fe_3O_4$/MWCNTs/β-CD/GCE (d). Hypoxanthine concentration: 1 μmol $L^{-1}$; scan rate: 100 mV $s^{-1}$.

The influence of pH on the response of the $Fe_3O_4$/MWCNTs/β-CD modified electrode has been investigated in the pH range from 6.0 to 9.0. As shown in Fig. 4, the direct electrochemistry response of hypoxanthine at modified electrode showed a strong dependence

on the pH value of 0.1 mol $L^{-1}$ PBS. The current intensity of the modified electrode improved gradually with the increase of the pH value from 6.0 to 7.5 and decreased with the pH further increased. Hence, a pH of 7.5 was selected in the subsequent hypoxanthine detection. In addition, the influence of pH on peak potential was studied. It was suggested that the oxidation peak potential shifted negatively with increasing solution pH, obeying the equation $E_p$ (V) = 1.5038–0.058 pH with $R^2$ = 0.9914. The slope of −58 mV $pH^{-1}$ is approximately close to the theoretical value of –59 mV $pH^{-1}$, which indicated that the number of protons and electrons involved in the oxidation of hypoxanthine was equal.

Fig. 5 shows the cyclic voltammograms of hypoxanthine at modified electrode in 0.1 mol $L^{-1}$ PBS at different scan rates. The oxidation peak potential was observed to shift positively with the increase in scan rate, and the peak currents increased linearly with the scan rate in the range of 20–200 mV $s^{-1}$. These indicated that the oxidation of hypoxanthine on the $Fe_3O_4$/MWCNTs/β-CD modified electrode is a typical adsorption-controlled process. The oxidation peak potential and ln $\nu$ showed a linearship and the regression equation can be expressed as $E_{pa}$ (V) = 0.0206 ln $\nu$ (V $s^{-1}$) + 1.065($R^2$ = 0.9942). As for an adsorption-controlled and irreversible electrode process, according to Laviron, $E_{pa}$ is defined by the following equation [29]:

$$E_{pa} = E^0 + (RT/\alpha nF)\ln(RTk^0/\alpha nF) + (RT/\alpha nF)\ln\nu$$

generally, $\alpha$ is assumed to be 0.5 in the totally irreversible electrode process. Hence, the number of electron transfer was calculated to be 2.4, indicating that two electrons were involved in the oxidation process. According to the previous result, the electrochemical oxidation of hypoxanthine on $Fe_3O_4$/MWCNTs/β-CD modified electrode undergoes a two electron and two proton reaction, and the electrochemical reaction of hypoxanthine can be described in Fig. 6.

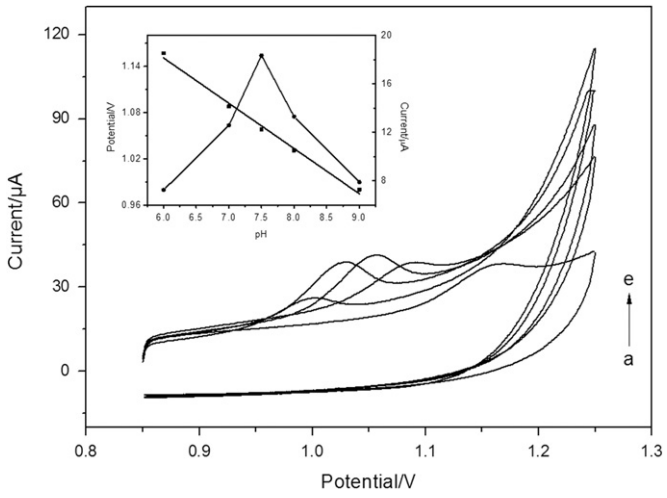


**Fig. 4.** Cyclic voltammograms at $Fe_3O_4$/MWCNTs/β-CD modified electrode in 0.1 mol $L^{-1}$ PBS at different pH values. From (a) to (e): 6.0, 7.0, 7.5, 8.0, and 9.0, respectively. Inset: effect of pH value on potentials (■) and current of hypoxanthine (●). Hypoxanthine concentration: 1 μmol $L^{-1}$; scan rate: 100 mV $s^{-1}$.

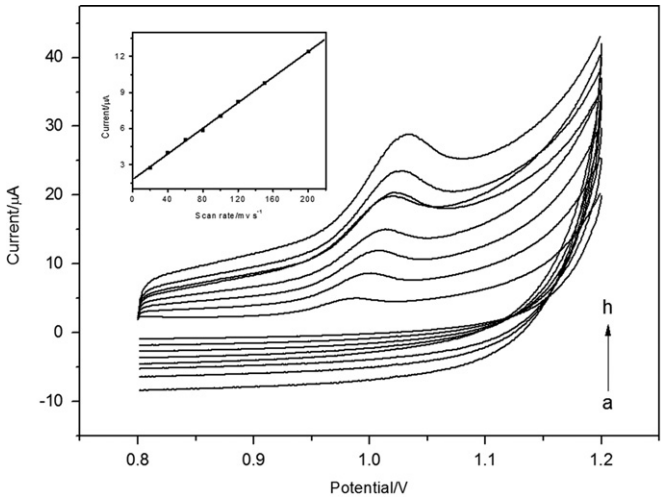


**Fig. 5.** Cyclic voltammograms of $Fe_3O_4$/MWCNTs/β-CD modified electrode in 0.1 mol $L^{-1}$ PBS (pH 7.5) at different scan rates. From (a) 20, (b) 40, (c) 60, (d) 80, (e) 100, (f) 120, (g) 150, and (h) 200 mV $s^{-1}$. Inset: the plot of peak current of hypoxanthine versus the scan rate from 20 to 200 mV $s^{-1}$. Hypoxanthine concentration: 1 μmol $L^{-1}$.

### 3.3. *Sequential injection lab-on-valve system with voltammetric detection*

Accumulation potential can improve the amount of hypoxanthine absorbed at the electrode surface, and then increase sensitivity and decrease detection limit. Therefore, the effect of accumulation potential on the current intensity was investigated ranging from –0.4 to 0.2 V at a fixed accumulation time of 120 s. With accumulation potential shifting from −0.4 to −0.1 V, the oxidation peak current increased gradually and the maximum was obtained at −0.1 V. After that, the peak current decreased with the further positive shift of accumulation potential. Thus −0.1 V was selected as an optimal accumulation potential. The influence of the accumulation was optimized using a defined flow rate and different sample volumes. It was found that the oxidation peak current increased gradually with accumulation time up to 120 s at an accumulation potential of −0.1 V, because more hypoxanthine could be adsorbed at the electrode surface with extending the accumulation time. With further improvement of the accumulation time above 120 s, the peak current was kept constant. This phenomenon could be attributed to the saturated adsorption of hypoxanthine at the electrode surface. Considering both sensitivity and work efficiency, the optimal accumulation time of 120 s was employed in further experiments.

Three of the most important cyclodextrins are α-CD, β-CD, and γ-CD in the order of increased size. The relatively rigid macrocyclic structure of β-CD strongly affects the surrounding water ordering, resulting in a decrease of the configurational entropy. Hence, the well-known anomaly of the β-CD water solubility obtained was 9 and 11 times more soluble compared with those of α-CD and γ-CD. This leads us to use β-CD to improve the resolvable property of MWCNTs. The effect of the amount of β-CD on the electrochemical behavior of hypoxanthine was studied. This can be controlled by using the same volume of DMF with different amounts of β-CD. The results indicated that the oxidation peak current was increased by increasing the amount of β-CD from 4 to 10 mg. Further increase caused a gradual decrease in the peak current of hypoxanthine, which could possibly be related to the increased film thickness. As a result, 10 mg of β-CD was selected as the optimum amount for the preparation of the modified electrode.

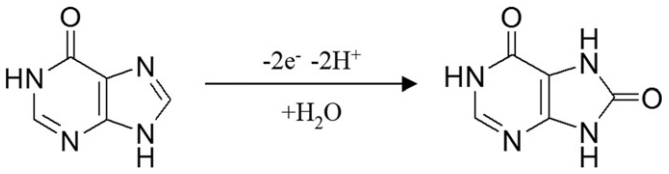


**Fig. 6.** Oxidation mechanism of hypoxanthine.

The amount of $Fe_3O_4$/MWCNTs/β-CD suspension could directly affect the current intensity through the film thickness of the MWCNTs/$Fe_3O_4$/β-CD modified electrode. In this study, the amounts of 2, 3, 4, 5, 6, and 7 μL of $Fe_3O_4$/MWCNTs/β-CD suspension were investigated by a linear sweep voltammetry. For $Fe_3O_4$/MWCNTs/β-CD amount lower than 4 μL, the anodic stripping current of hypoxanthine increased with the increasing amount of suspension, which may be due to an increase in the adsorption of hypoxanthine on the electrode surface. However, for $Fe_3O_4$/MWCNTs/β-CD amount higher than 4 μL, the thicker film of the $Fe_3O_4$/MWCNTs/β-CD at the electrode surface will decrease the conductivity and hinder the electron transfer, and then the anodic stripping current of hypoxanthine decreased gradually. Thus, 4 μL was chosen as the optimal amount of $Fe_3O_4$/MWCNTs/β-CD.

The effect of flow rate on the analytical signal was evaluated. The current increased with the flow rate until 16 μL $s^{-1}$ and then decreased sharply for higher values. The results indicated that a higher sample flow rate may cause less dispersion on the surface of the electrode, which was contributed to enhance the current intensity. Conversely, the $Fe_3O_4$/MWCNTs/β-CD film on the electrode surface could be deteriorated at higher flow rate range. For this reason, a flow rate of 16 μL $s^{-1}$ was used throughout this work.

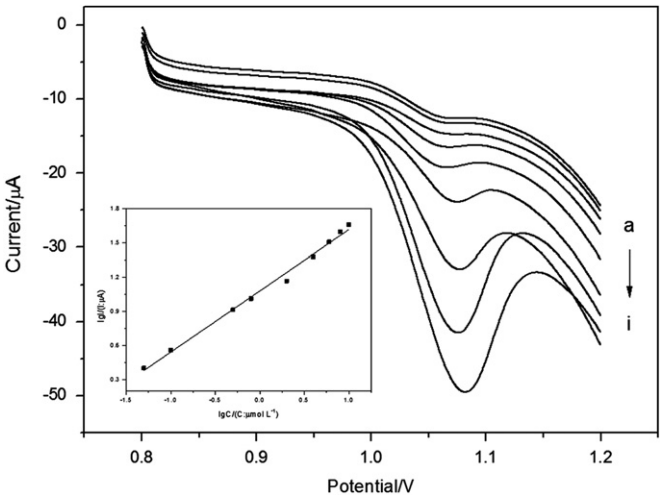


**Fig. 7.** Voltammograms obtained at the modified electrode with increasing concentration of hypoxanthine. (a) 0.05, (b) 0.1, (c) 0.5, (d) 0.8, (e) 2, (f) 4, (g) 6, (h) 8, and (i) 10 μmol $L^{-1}$. Inset: calibration plot of log peak current versus log hypoxanthine concentration.

### 3.4. Interference studies

In order to demonstrate the selectivity of the developed method for the determination of hypoxanthine, various potential organic compounds and inorganic ions were added to the solution containing $1.0\times10^{-6}$ mol $L^{-1}$ hypoxanthine and the recommended procedure for sample analysis was applied. Tolerance limit was defined as the ratio of interference to hypoxanthine for a $\pm$5.0% signal change. It was found that 500-fold concentration of $SO_4^{2-}$, $Cl^-$, and $NO_3^-$, 200-fold of glucose, vitamin C, glutamic acid, *L*-homocysteine, vitamin B1, vitamin B2, and phenol, 100-fold of uric acid, and ascorbic acid, 50-fold of xanthine and adenine have no influence on the signals of hypoxanthine. Otherwise, some metal ions such as 500-fold of $Fe^{3+}$, $Zn^{2+}$, $Al^{3+}$, $Mn^{2+}$, $Ca^{2+}$, and $Ba^{2+}$ have no influence on the determination of hypoxanthine. The interference of other substances with similar structures (catechol and resorcin) was also studied because their anodic peak overlapped with the peak of hypoxanthine, and the maximum allowable concentration could be tolerated at 50-fold. When the meat sample was treated with appropriate dilution, the concentrations of major matrix species were unlikely to exceed the maximal permissible values, so that common substances caused no significant interference with hypoxanthine during analysis. Therefore, this method demonstrated good selectivity and could be used to analyse hypoxanthine directly without masking reagents or further pretreatments.

### 3.5. Analytical performances and method validation

All the experimental parameters were carefully optimized using univariate approach. The inserted plots in Fig. 7 show the calibration curve of the modified electrode under the optimal experimental conditions. It was found that there was a linear relationship between the log current intensity and the log hypoxanthine concentrations over the range from $5.0\times10^{-8}$ to $1.0\times10^{-5}$ mol $L^{-1}$. The linear regression equation was $\lg I_p = 0.5379 \lg C + 1.080$, where $I_p$ is the current intensity (μA), $C$ is the hypoxanthine concentration (μmol $L^{-1}$), and the coefficient is 0.9965. According to the IUPAC definition, the lower detection limit is $0.3\times10^{-8}$ mol $L^{-1}$. The result was calculated with the equation $LOD = 3S_b/m$, where $S_b$ is the standard deviation of the blank measurements ($n=11$) and $m$ is the slope of the calibration graph. The repeatability of the sensor was estimated by voltammetric measurement of $1.0\times10^{-6}$ mol $L^{-1}$ hypoxanthine, and the relative standard deviation (*RSD*) was 3.8% ($n=11$), revealing that this method had good reproducibility. The sampling frequency was 20 $h^{-1}$ in the current condition. Moreover, the peak current began to drop after approximately 20 cycles, which indicated that the modified electrode surface was stable for dealing with the deposition and stripping procedure for 20 times.

We compared our method with the other modified electrodes reported earlier in the literatures [4–9,30–33]. As listed in Table 1, the established method exhibits wider linear range and lower detection limit. Moreover, this on-line SI-LOV method provided a high degree of automation in terms of integration and flexibility, reduced the risk of sample contamination and required smaller volumes of solution.

The practical application of the fabricated $Fe_3O_4$/MWCNTs/β-CD modified electrode was used to determine hypoxanthine in fish and pork samples. All the samples were diluted to fit the linear range of hypoxanthine, and the current response was recorded. Table 2 listed the data of hypoxanthine determination by $Fe_3O_4$/MWCNTs/β-CD modified electrode in different samples, from which satisfactory results were obtained. The recoveries were in the range from 97.5% to 103.2%, indicating that this proposed electrochemical method can be reliably applied in the determination of hypoxanthine. Moreover, the results gained from the present method and those from the HPLC method were also compared and presented in Table 2. For HPLC analysis, the sample solutions were analyzed under the following conditions: methanol–water (8:92, v/v) was used as the mobile phase at a flow rate of 1 mL $min^{-1}$; UV detector wavelength was set at 249 nm; and sample injection was 20 μL. The peak retention time for the elution of hypoxanthine was 6.98 min. The concentration values obtained from the two methods were compared with paired *t*-test statistical approach. The calculated *t*-test values did not exceed the theoretical values at the 95% confidence level, indicating that there was no significant difference between these two analytical methods.

## 4. Conclusions

In this study, we have prepared and explored $Fe_3O_4$/MWCNTs/β-CD modified electrode in the sequential injection lab-on-valve system for the rapid identification and highly sensitive detection of hypoxanthine. Cyclic voltammetry was used to investigate the electrocatalytic ability of hypoxanthine and linear sweep

**Table 1**
Comparison of different modified electrodes for hypoxanthine determination.

| Electrodes | Linear range ($\mu$mol $L^{-1}$) | Detection limit ($\mu$mol $L^{-1}$) | Methods | System | Ref. |
|---|---|---|---|---|---|
| Hydroxymethylferrocene modified carbon paste electrode | 0.6–700 | 0.6 | Amperometry | Batch | [4] |
| Osmium–polyvinylpyridine gel polymer and xanthine oxidase bienzyme modified glassy carbon electrode | 0.5–80 | 0.2 | Amperometry | Batch | [5] |
| Sodium montmorillonite–methyl viologen carbon paste modified electrode | 1–400 | 0.8 | Cyclic voltammetry | Batch | [6] |
| Graphene sheets with water-soluble conducting graft copolymer modified electrode | 0.03–28 | 0.001 | Amperometry | Batch | [7] |
| Multi-wall carbon nanotubes–dicetyl phosphate film modified vitreous carbon electrode | 0.5–200 | 0.2 | Linear scan voltammetry | Batch | [8] |
| Mesoporous $TiO_2$ modified electrode | 0.2–50 | 0.05 | Square wave voltammetry | Batch | [9] |
| Xanthine oxidase on nanocrystal gold–carbon paste electrode | 0.5–10 | 0.1 | Amperometry | Batch | [30] |
| Silk broin/cellulose acetate membrane electrode incorporating xanthine oxidase | 0.1–10 | 0.1 | Amperometry | Batch | [31] |
| Poly (pyrocatechol violet)/functionalized multi-walled carbon nanotubes composite film modified electrode | 0.5–90 | 0.2 | Differential pulse voltammetry | Batch | [32] |
| A glassy carbon electrode modified with as commercially received multiwalled carbon nanotubes | up to 700 | 0.141 | Differential pulse voltammetry | Batch | [33] |
| MWCNTs/$Fe_3O_4$/β-CD modified glassy carbon electrode | 0.05–10 | 0.003 | Linear sweep voltammetry | Automatic | This work |

**Table 2**
Determination of hypoxanthine in meat samples.

| Sample | Original[a] ($\mu$mol $L^{-1}$) | Spiked ($\mu$mol $L^{-1}$) | Found[a] ($\mu$mol $L^{-1}$) | HPLC[a] ($\mu$mol $L^{-1}$) | Recovery (%) |
|---|---|---|---|---|---|
| Fish 1 | $4.14 \pm 0.011$ | 1.00 | $5.09 \pm 0.011$ | $4.09 \pm 0.070$ | 99.1 |
| | | 2.00 | $6.19 \pm 0.090$ | | 101.5 |
| Fish 2 | $3.39 \pm 0.010$ | 1.00 | $4.41 \pm 0.009$ | $3.50 \pm 0.057$ | 100.8 |
| | | 2.00 | $5.34 \pm 0.013$ | | 98.7 |
| Pork 1 | $1.00 \pm 0.013$ | 0.500 | $1.54 \pm 0.033$ | $0.97 \pm 0.028$ | 103.2 |
| | | 1.00 | $2.01 \pm 0.061$ | | 99.8 |
| Pork 2 | $1.26 \pm 0.044$ | 0.500 | $1.73 \pm 0.057$ | $1.30 \pm 0.012$ | 97.5 |
| | | 1.00 | $2.29 \pm 0.034$ | | 102.4 |

[a] Mean and standard deviation for 3 determinations.

voltammetry was used for the quantification of hypoxanthine. The response of the modified electrode to hypoxanthine exhibited a good analytical performance in comparing with bare electrode, which has a considerable effect on improvement selectivity and decrease of the voltammetric detection limit. The flow strategy could provide a simple and rapid way for hypoxanthine quantification with high sensitivity. Meanwhile, if the lab-on-valve system is equipped with an effective solid-phase extraction column, to eliminate interfering substance from the complex matrix samples, this can be expected to expand the applicability of the proposed method to a considerable extent.

## Acknowledgments

This work was supported by the National Natural Science Foundation of China (20875081), the Key Laboratory Foundation of Environmental Material and Engineering of Jiangsu Province (JHCG201004), the Innovative Project Foundation of Yangzhou University (2011CXJ015), and a Project Funded by the Priority Academic Program Development of Jiangsu Higher Education Institutions.

## References

[1] A.S. Hernández-Cázares, M.C. Aristoy, F. Toldrá, Food Chem. 123 (2010) 949.
[2] M. Numata, N. Funazaki, S. Ito, Y. Asano, Y. Yano, Talanta 43 (1996) 2053.
[3] A. Câmpean, M. Tertiș, R. Săndulescu, Cent. Eur. J. Chem. 9 (2011) 466.
[4] H. Okuma, H. Takahashi, S. Sekimukai, K. Kawahara, R. Akahoshi, Anal. Chim. Acta 244 (1991) 161.
[5] L.Q. Mao, K. Yamamoto, Anal. Chim. Acta 415 (2000) 143.
[6] S.S. Hu, C.L. Xu, J.H. Luo, J. Luo, D.F. Cui, Anal. Chim. Acta 412 (2000) 55.
[7] J. Zhang, J.P. Lei, R. Pan, Y.D. Xue, H.X. Ju, Biosens. Bioelectron. 26 (2010) 371.
[8] S.F. Lü, Anal. Sci. 19 (2003) 1309.
[9] X.F. Xie, K.F. Yang, D. Sun, Colloids Surf. B 67 (2008) 261.
[10] H.S. Yin, Y.L. Zhou, Q. Ma, S.Y. Ai, Q.P. Chen, L.S. Zhu, Talanta 82 (2010) 1193.
[11] H.S. Yin, L. Cui, Q.P. Chen, W.J. Shi, S.Y. Ai, L.S. Zhu, L.N. Lu, Food Chem. 125 (2011) 1097.
[12] Y. Zhang, G.M. Zeng, L. Tang, D.L. Huang, X.Y. Jiang, Y.N. Chen, Biosens. Bioelectron. 22 (2007) 2121.
[13] S.F. Wang, Y.M. Tan, Anal. Bioanal. Chem. 387 (2007) 703.
[14] C.M. Yu, J.W. Guo, H.Y. Gu, Microchim. Acta 166 (2009) 215.
[15] H. Fan, Z.Q. Pan, H.Y. Gu, Microchim. Acta 168 (2010) 239.
[16] F. Valentini, S. Orlanducci, M.L. Terranova, A. Amine, G. Palleschi, Sensors Actuators B 100 (2004) 117.
[17] J. Wang, S.B. Hocevar, B. Ogorevc, Electrochem. Commun. 6 (2004) 176.
[18] J.P. Salvetat, J.M. Bonard, N.H. Thomson, A.J. Kulik, L. Forró, W. Benoit, L. Zuppiroli, Appl. Phys. A 69 (1999) 255.
[19] C.L. Bian, Q.X. Zeng, L.J. Yang, H.Y. Xiong, X.H. Zhang, S.F. Wang, Sensors Actuators B 156 (2011) 615.
[20] S. Qu, J. Wang, J.L. Kong, P.Y. Yang, G. Chen, Talanta 71 (2007) 1096.
[21] J. Szejtli, Chem. Rev. 98 (1998) 1743.
[22] Q. Shen, X.M. Wang, J. Electroanal. Chem. 632 (2009) 149.
[23] G. Chambers, C. Carroll, G.F. Farrell, A.B. Dalton, M. McNamara, M. in het Panhuis, H.J. Byrne, Nano Lett. 3 (2003) 843.
[24] M.D.L. de Castro, J. Ruiz-Jimenez, J.A. Perez-Serradilla, Trends Anal. Chem. 27 (2008) 118.
[25] M. Miró, E.H. Hansen, Anal. Chim. Acta 600 (2007) 46.
[26] J.H. Wang, E.H. Hansen, Trends Anal. Chem. 22 (2003) 225.
[27] Y. Wang, X.Y. Luo, J. Tang, X.Y. Hu, Q. Xu, C. Yang, Anal. Chim. Acta 713 (2012) 92.
[28] L.R. Kong, X.F. Lu, W.J. Zhang, J. Solid State Chem. 181 (2008) 628.
[29] E. Laviron, J. Electroanal. Chem. Interfacial Electrochem 101 (1979) 19.
[30] L. Agüí, J. Manso, P. Yáñez-Sedeño, J.M. Pingarrón, Sensors Actuators B 113 (2006) 272.
[31] C. Qiong, T.Z. Peng, L.J. Yang, Anal. Chim. Acta 369 (1998) 245.
[32] Y. Wang, Colloids Surf. B 88 (2011) 614.
[33] A.S. Kumar, R. Shanmugam, Anal. Methods 3 (2011) 2088.